Paper:
Riza Putra, B., Carta, M., Malpass-Evans, R., McKeown, N. & Marken, F. (2017). Potassium cation induced ionic diode blocking for a polymer of intrinsic microporosity | nafion “heterojunction” on a microhole substrate. *Electrochimica Acta, 258*, 807-813.
http://dx.doi.org/10.1016/j.electacta.2017.11.130

REVISION 2

17th November 2017

Potassium Cation Induced Ionic Diode Blocking for a Polymer of Intrinsic Microporosity | Nafion "Heterojunction" on a Microhole Substrate

Budi Riza Putra [1,2], Mariolino Carta [3], Richard Malpass-Evans [3], Neil B. McKeown [3], and Frank Marken*[1]

[1] *Department of Chemistry, University of Bath, Claverton Down, BA2 7AY, UK*

[2] *Department of Chemistry, Faculty of Mathematics and Natural Sciences, Bogor Agricultural University, Bogor, West Java, Indonesia*

[3] *School of Chemistry, University of Edinburgh, Joseph Black Building, West Mains Road, Edinburgh, Scotland EH9 3JJ, UK*

To be submitted to Electrochimica Acta (Special Issue ECHEMS 2017)

Proof to F. Marken (f.marken@bath.ac.uk)

Abstract

"Heterojunction" ionic diodes based on a Nafion cation conductor and a polymer of intrinsic microporosity (PIM) interfaced at a 6 μm thickness polyethylene-terephthalate (PET) film with 20 μm diameter microhole exhibit rectification effects in cation (K^+) flux. When combined with the precipitation reaction of potassium cations with perchlorate anions to give insoluble $KClO_4$ (solubility product ca. 1.05×10^{-2} M^2 at 25 °C) at the PIM | Nafion interface, inversion of the rectification/diode effect occurs and the formerly "open" state changes into a "closed" state due to blocking of ion flow. The localised interfacial precipitation reaction is due to up to three orders of magnitude accumulation of K^+ at the PIM | Nafion interface and shown to be fast and reversible. The effects of K^+/ClO_4^- concentration and of Na^+ interference are considered. The blocking process within the heterojunction ionic diode is suggested to be dynamic/fast and potentially useful as a diode sensor mechanism based on solubility product dependent precipitation.

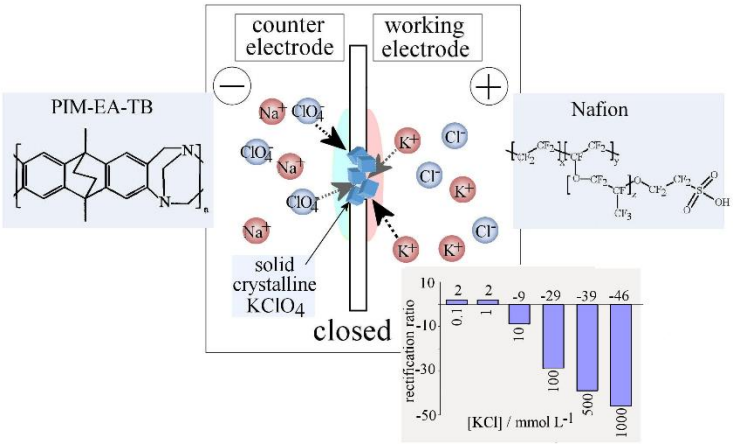

Keywords: membrane; sensor; precipitation; voltammetry; potassium

1. Introduction

Polymer interfaces provide interesting reaction environments [1,2] related (at least a little bit at functional level) to biological membrane interfaces, where the flux of ions can trigger chemical reactions and *vice versa* (e.g. in ATPases [3]). We have recently investigated polymer interfaces in microhole "heterojunctions" [4] where cation flux driven by applied potential is high in one direction but low in the opposite direction. The resulting rectification or "ionic diode" effect can be substantial and optimisation of this effect has been suggested to lead to new desalination [5] and energy harvesting [6] technology. The applied potential-dependent reaction conditions at these polymer micro-interfaces are of interest in view of chemical reactions that can be triggered and electrochemical mechanisms that may contribute to sensor development. Here a process sensitive to potassium, K^+, is investigated.

The emerging field of ionic diode devices [7,8] has initially been based mainly on gel-electrolyte interfaces [9], which led to ionic rectifier [10] and amplifier [11] processes based on ionic currents. Today, the ionic diode field is dominatd by nanochannel [12], nanocone [13,14], and nanopore [15,16] devices that mimic much more closely the biological ion channels located in membranes [17]. A wide range of nano-architectures [18,19] and applications [20] has been proposed, pH-switchable devices have been developed [21], and a perspectives review has appeared with focus on stimuli response "iontronics" [22]. Recently, when investigating microporous polymers, we observed micro-scale ionic diode behaviour also for asymmetrically deposited ionomers on microholes in poly-ethylene-terephthalate (PET) substrates [23]. Both "cationic diodes" or "anionic diodes" (with cation or anion charge carriers, respectively) were observed with the microporous ionomer based on either Nafion [24], cellulose or modified cellulose [25,26], or on

polymers of intrinsic microporosity (PIMs) containing amines, which when protonated provide intrinsic positive charges [27].

Polymers of intrinsic microporosity (PIMs) offer a novel class of highly porous materials with excellent processibility [28,29]. The molecular structure of these materials is based on a highly rigid and contorted polymer/molecular chain that prevents packing and ensures microporosity [30]. Important examples have been PIM-1 [31] and Tröger Base PIMs [32]. Materials such as PIM-EA-TB (EA = ethanoanthracene and TB = Tröger base, see molecular structure in Figure 1) have been developed with tertiar amine functionality in the backbone [33]. Most applications proposed for PIMs have been in gas separation [34,35] and storage [36], but interesting new applications now also emerged in organocatalysis [37], electrochemistry [38,39,40], reagentless electro-chemiluminescence [41], and in energy storage [42].

We have recently demonstrated that a Nafion film deposited asymmetrically onto a microhole (in PET) is sufficient to trigger ionic diode phenomena [43] and that a PIM-EA-TB deposit opposite to the Nafion can help improving ionic diode perfomance as well as defining a PIM-EA-TB | Nafion interface [4]. The PIM-EA-TB | Nafion heterojunction interface (Figure 1A) is employed here in a new way. The Nafion deposit ensures "cationic diode" characteristics and the case of K^+ cations in the electrolyte is investigated. The PIM-EA-TB deposit allows precipiation reactions to occur in a defined interfacial region. The accummulation of K^+ at the PIM-EA-TB | Nafion interface is exploited in a precipitation reaction with perchlorate, ClO_4^-, to give "inverted" diode characeristics leading to sensor applications.

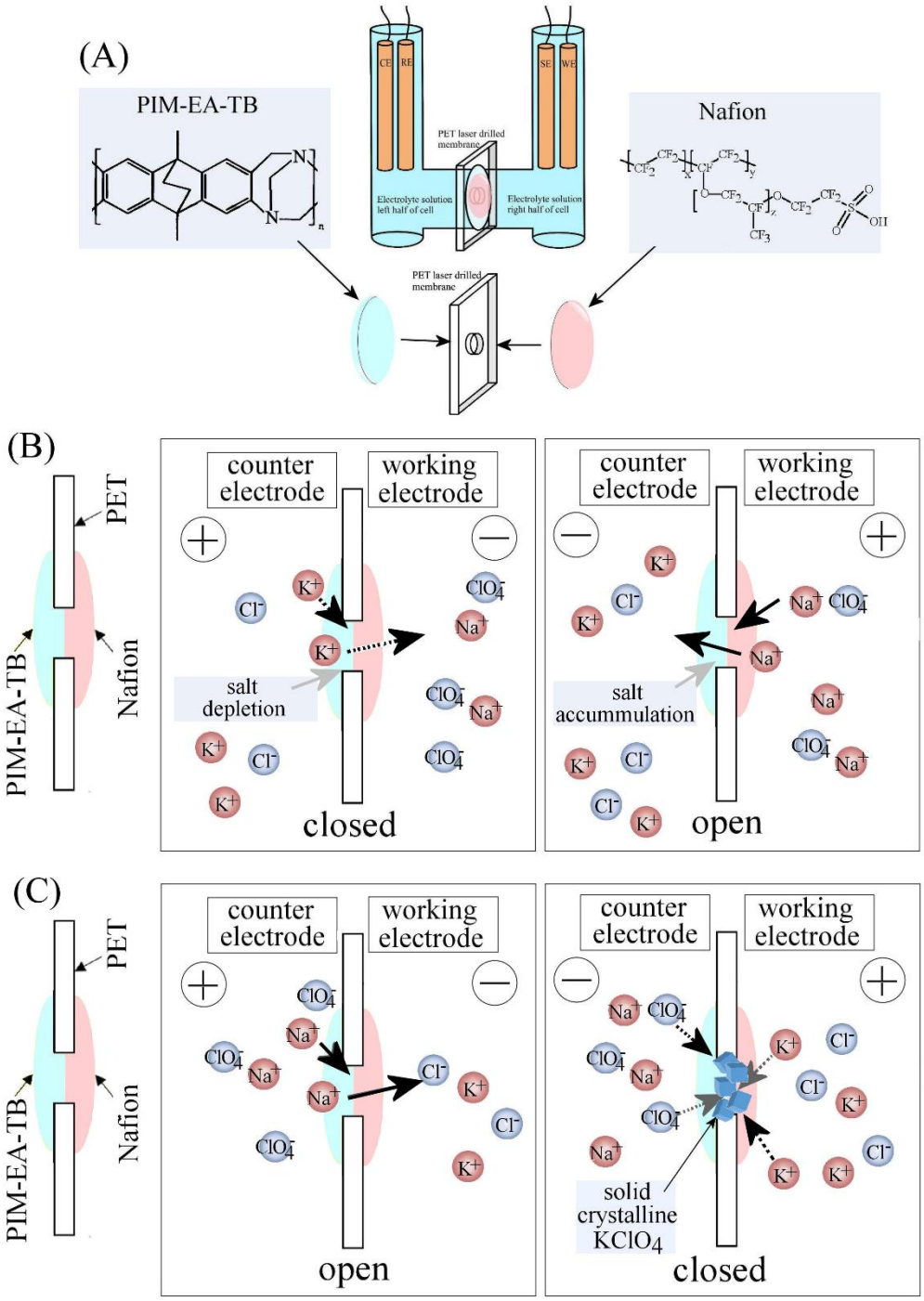

Figure 1. (A) Schematic drawing of the two-compartment four-electrode electrochemical cell with a microhole interface separator. For heterojunction experiments Nafion is applied on the working electrode side and PIM is applied on the counter electrode side. (B) Operational scheme for the "normal" cationic diode effect. (C) Operational scheme for the "inverted" cationic diode effect with $KClO_4$ precipitation and blocking.

2. Experimental

2.1. Chemical Reagents. Nafion®-117 (5% in a mixture of lower aliphatic alcohol and water), potassium chloride, sodium perchlorate, agarose, and sodium chloride were obtained from Sigma-Aldrich or Fisher Scientific and used without further purification. Solutions were prepared under ambient conditions in volumetric flasks with ultra-pure water of resistivity 18.2 MΩ cm from an ELGA Purelab Classic system.

2.2. Instrumentation. Electrochemical data (for both voltammetry and chronoamperometry) were recorded at $T = 20 \pm 2$ °C on a potentiostat system (Ivium Compactstat, Netherlands). A classic 4-electrode electrochemical cell similar to that employed in previous membrane conductivity studies [4] was used. The membrane separates two tubular half-cells (12 mm diameter, see Figure 1), one with Pt wire working and KCl-saturated calomel (SCE) sense electrode and the other with SCE electrode and Pt wire counter electrode. In electrochemical measurements the working electrode was always located on the side of the Nafion film.

2.3. Heterojunction Formation. The procedure follows that reported recently [4]. Briefly, polyethylene-terephthalate (PET) films of 6 μm thickness with 20 μm diameter microhole were obtained from Laser-Micro-Machining Ltd., Birmingham, UK. A glass slide was pre-coated with a film of 1% agarose gel and the PET film placed onto the gel (to define the interface within the microhole). A 10 μL volume of PIM-EA-TB solution (2% in chloroform) was applied to the surface and with a glass rod the PIM-EA-TB solution was spread evenly over the PET surface to give approximately 1 cm^2 film (to give PIM-EA-TB with approximately 10 μm thickness [4]). After drying the PET film was turned around and coated with a volume of 10 μL Nafion solution from the oppostie side (to give Nafion with approximately 6 μm thickness [4]). The film was mounted between the two glass flanges with the help of some Dow-Corning vacuum grease.

3. Results and Discussion

3.1. PIM-EA-TB | Nafion Heterojunction Deposits I.: Characterisation of "Normal" Cationic Diode Effects. The ionic diode "heterojunction" architecture has been recently reported as based on a 6 μm thick PET film with a 20 μm diameter laser-drilled hole [4]. Nafion (ca. 6 μm thickness) and PIM-EA-TB (ca. 10 μm thickness are applied to opposite sides. Ionic diode phenomena (or ion flux rectification phenomena) have been observed first with asymmetrically deposited ionomers such as Nafion [24] or cellulose [25]. The heterojunction approach reported here is governed mainly by the Nafion cation conductor (see Figure 2A) to induce semipermeability and a low resistance to cation flow in the open state of the diode. The effect of the PIM-EA-TB deposited opposite to the Nafion is mainly to modify the transport conditions towards the microhole (here 20 μm diameter) in the closed state of the diode. The second polymer also helps defining a stable interface for precipitaion reactions to occur as is shown below.

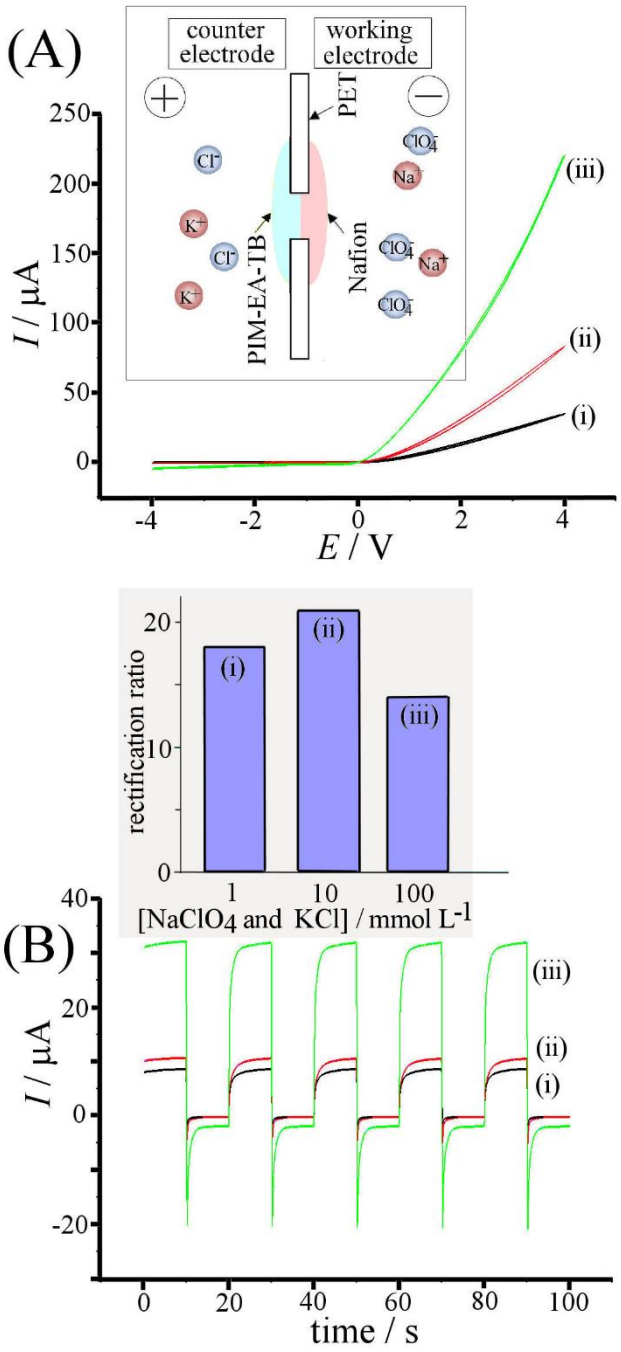

Figure 2. (A) Cyclic voltammograms (scan rate 25 mVs^{-1}) for a PIM-EA-TB | Nafion hetero-junction with (i) 1 mM, (ii) 10 mM, (iii) 100 mM KCl (counter electrode compartment) and $NaClO_4$ (working electrode compartment) electrolyte. Inset showing the cell configuration. (B) Chronoamperometry data switching between +1 V and -1V. Inset showing the rectification ratio of currents at +/-1 V.

Figure 2A shows voltammetry data for the case of fast Na^+ transport in the open state of the diode (positive applied potential on the Nafion side) and inhibited K^+ transport in the closed state of the diode (negative applied potential on the Nafion side). A schematic description of the processes is shown in Figure 1B with the main mechanistic feature indicated as salt depletion ("closed") and salt accumulation ("open") [43]. Data in Figure 2A show currents with rectifier characteristics with positive potential applied (the diode is "open"). The magnitude of the current in this state is affected by the electrolyte concentration. Based on recent studies [24,43] this is likely to be mainly a reflection of Na^+ conductivity within the Nafion deposit in the open state of the diode.

With negative applied potentials (in the "closed" state of the ionic diode) K^+ transport occurs, but only at a low level with a resulting rectification ratio (calculated as the ratio of currents I(+1V)/I(-1V)) of typically 20 (see Figure 2B). Complementary chronoamperometry data in Figure 2B are consistent with voltammetry data in Figure 2A and mainly reflect the switching time (time constant) of the diode, which can be estimated here as typically 1 s. This time constant is linked to the development of the diffusion-migration layer within the PIM-EA-TB film or within the Nafion layer [21]. The fact that there are two different anions, perchlorate and chloride, in the electrolye media in the right and left half-cells does not affect the mechanism of the cationic diode, which is dependent solely on sodium cation transport in the open state and potassium cation transport in the closed state. Next, the two electrolyte solutions right and left are exchanged.

3.2. PIM-EA-TB | Nafion Heterojunction Deposits II.: "Inverted" Cationic Diode Effects and KCl Concentration Effects. By switching the electrolyte solution between the two compartments of the measurement cell the KCl solution is now in contact to the Nafion film (see Figure 3A). This results in a change in cation flow from dominated by Na^+ flow to now dominated by K^+ flow. In the open state of the diode, K^+ is conducted through the Nafion into the opposite compartment with $NaClO_4$ solution. Under these conditions, the K^+-enrichment of the interfacial region in the microhole is anticipated [43]. In order to investigate the effects of K^+ precipitating with ClO_4^- under these conditions, the concentration of $NaClO_4$ is fixed at 100 mM in the external electrolyte

solution. Aqueous $NaClO_4$ can permeate through PIM-EA-TB and it can be assumed that the concentration of $NaClO_4$ within the electrolyte and within the PIM-EA-TB (with 1-2 nm pore size [23]) are similar. Although, the exact concentration of $NaClO_4$ within the PIM is currently not known.

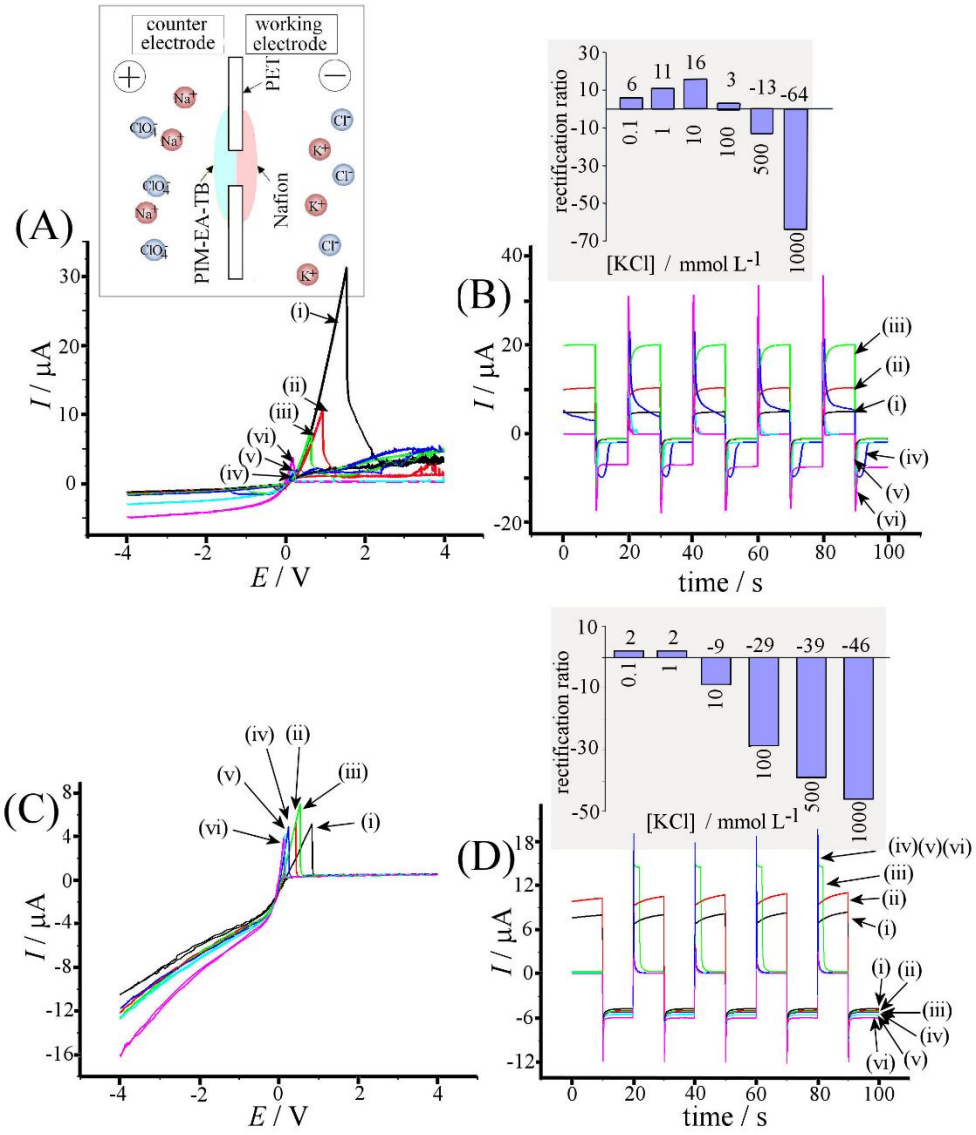

Figure 3. (A) Cyclic voltammograms (scan rate 25 mVs^{-1}) for a PIM-EA-TB | Nafion hetero-junction with 100 mM $NaClO_4$ (counter electrode compartment) and (i) 0.1 mM, (ii) 1 mM, (iii) 10 mM, (iv) 100 mM, (v) 500 mM, (vi) 1000 mM KCl (working electrode compartment) electrolyte. Inset showing the cell configuration. (B) Chronoamperometry data switching between +1 V and -1V. Inset showing the rectification ratio at +/-1 V. (C) As above but with 500 mM $NaClO_4$. (D) As above, but with 500 mM $NaClO_4$.

Cyclic voltammograms in Figure 3A reveal new features in the positive potential domain. With only 0.1 mM KCl present the current rises to approximately 30 μA but then collapses and settles at a much lower level of about 3-4 μA. The current has superimposed a considerable noise. When increasing the concentration of aqueous KCl further to 1 mM and 10 mM, the current peak is lowered to approximately 11 μA and 8 μA, respectively. The current peak must be associated with the formation of insoluble $KClO_4$ (see Figure 1C) at the PIM-EA-TB | Nafion interface and the corresponding blocking of the ion flow. The observation that the "blocking potential" is lowered with higher KCl concentration suggests that the $KClO_4$ precipitation conditions are reached more readily in the presence of a higher concentration of KCl.

The fact that a peak associated with $KClO_4$ precipitation is observed suggests that the solubility product for $KClO_4$ is reached. For $KClO_4$ the solubility product is $K_{SP} = [ClO_4^-] \times [K^+] = 1.05 \times 10^{-2}$ mol^2 dm^{-6} at 25 ^oC [44]. The concentration of $NaClO_4$ within the microporous environment is likely to be approximately 0.1 mol dm^{-3}, close to the bulk electrolyte concentration. Therefore, the K^+ concentration at the PIM-EA-TB | Nafion interface at the moment when the peak is observed is likely to be close to 0.1 mol dm^{-3}. During the process denoted "open diode" in the positive applied potential domain cations from the KCl solution are accumulated into the Nafion film and "pushed" into the PIM-EA-TB environment to give locally much higher concentrations. Even for 0.1 mM K^+ in the external electrolyte the precipiation peak is observed. Therefore, a three order of magnitude accumulation effect of K^+ at the PIM-EA-TB | Nafion interface appears feasible.

When increasing the concentration of KCl even further the positive current (with positive applied potential) remains suppressed very effectively (with some superimposed noise indicative of dynamic phenomena in the $KClO_4$ blocking layer). At negative applied potentials a negative current is observed. This current is still consistent with the "closed" diode state, but now appears higher when compared to the blocked current with positive applied potentials. The rectification ratio is indeed inverted. The external KCl concentration at which inversion occurs (see Figure 3B) is approximately 100 mM.

Figure 3B shows chronoamperometry data with a much more complex behaviour when compared to data in Figure 2B. For a low concentration of KCl (see i-iii) the rectification ratio remains positive with transients shaped similarly to those observed in Figure 2B. For 100 mM KCl (see iv) a slow blocking transient is seen with positive applied potential. For 500 mM (see v) and 1000 mM KCl (see vi) the blocking transient becomes much faster. The rectification ratio reaches -64. Therefore a systematic KCl concentration dependent behaviour is observed associated with the formation of a blocking layer of $KClO_4$.

In Figure 3C and 3D are presented additional data for a fixed concentration of 500 mM $NaClO_4$ at the PIM-EA-TB side of the measurement cell. Figure 3C shows voltammetry data with a clear $KClO_4$ precipitation point. The higher perchlorate concentration lowers currents and decreases the voltage necessary for blocking. In Figure 3D chronoamperometry data show time-dependent switching/blocking of the diode at +1V and -1V applied ptential. For 500 mM $NaClO_4$, the KCl concentration at which inversion of the diode happens is lowered to approximately 10 mM (see Figure 3D inset).

The shape of the peaks during "blocking events" can be interpreted as the gradual formation of a physical barrier towards ion flow. In cyclic voltammograms a sharp decrease in current (Figure 3A) due to rapid nucleation and growth is sometimes followed by a more gradual "closing" of the barrier, presumably due to $KClO_4$ crystals inter-growing. A 100% blockage of K^+ transport is unlikely as this should result in the "re-opening" of the heterojunction due to $KClO_4$ dissolving back into solution. Therefore a more dynamic precipitation/dissolution process seems likely. It is interesting to note the current noise in the positive applied potential domain, which likely to be associated with fluctuations in the $KClO_4$ blocking layer.

3.3. PIM-EA-TB | Nafion Heterojunction Deposits III.: Sodium Cation Interference During $KClO_4$ Blocking. The formation of the $KClO_4$ blocking layer is caused by a precipitation reaction

at the location of the PIM-EA-TB | Nafion interface and is likely to be affected by the presence of other mobile cations. In order to explore effects of this nature NaCl has been added into the compartment containing KCl (the working electrode compartment with Nafion film, see Figure 4A inset). Now a competition of K^+ and Na^+ ion flux occurs through the Nafion film. The local concentration of K^+ at the PIM | Nafion interface is likely to be lowered at a given potential.

Data in Figure 4A show cyclic voltammetry experiments in the presence of 10 mM NaCl added and as a function of KCl concentration. When compared to data in Figure 3A the first observation is that the magnitude of currents has increased. The presence of additional Na^+ apperas to associated with additional cation flow across the Nafion film leading to higher currrents in the positive applied potential domain. The peak position (indicating the $KClO_4$ blocking) appears to shift more positive (i) at lower K^+ concentration and (ii) at increased Na^+ concentration (at least as an underlying trend with some exceptions). In the presence of 30 mM Na^+ (see Figure 4C) and for low K^+ concentrations the peak associated with $KClO_4$ blocking is too far in the positive potential range to be observed.

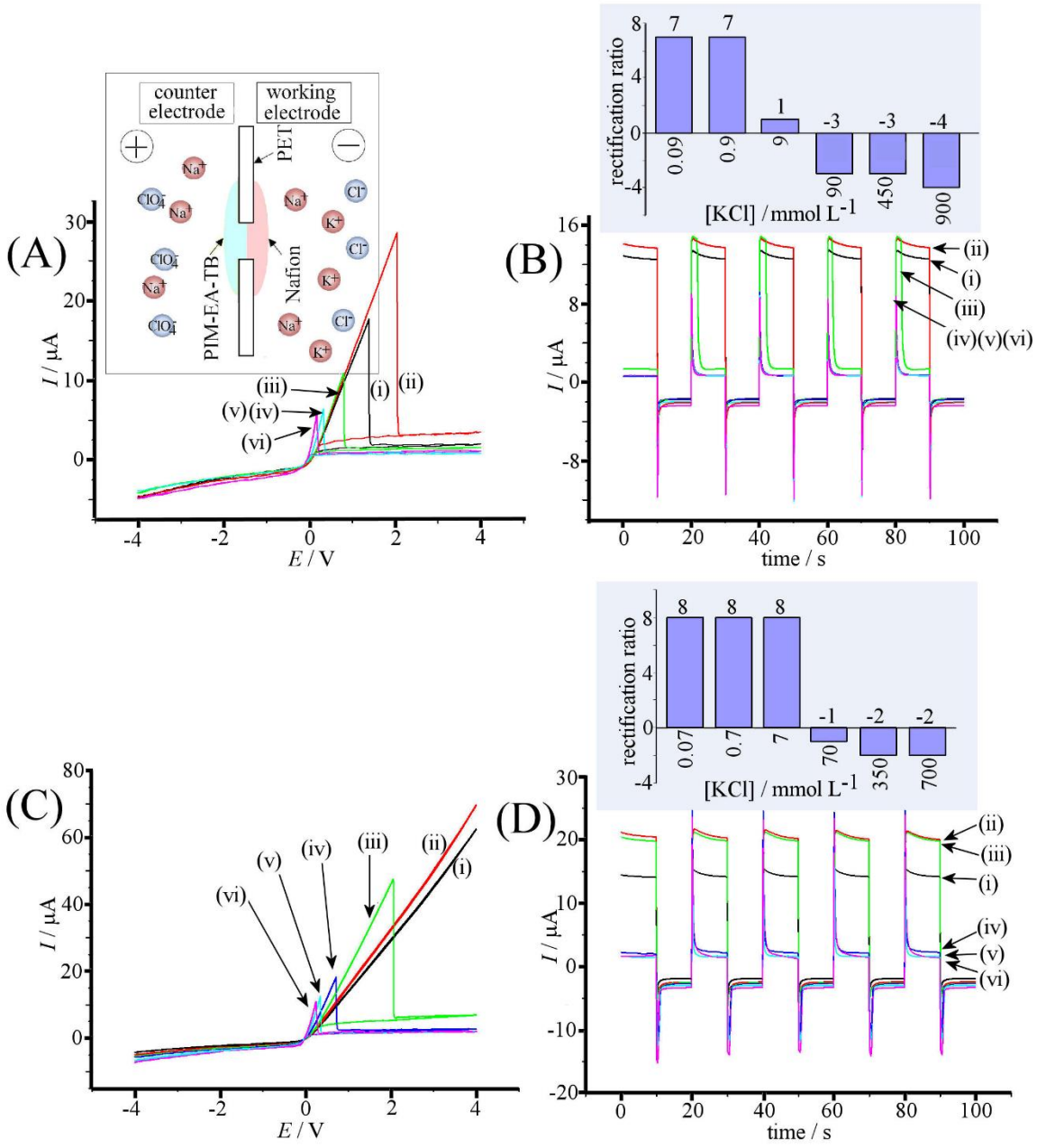

Figure 4. (A) Cyclic voltammograms (scan rate 25 mVs^{-1}) for a PIM-EA-TB | Nafion hetero-junction with 100 mM $NaClO_4$ and (i) 10 mM NaCl/0.09 mM KCl, (ii) 10 mM NaCl/0.9 mM KCl, (iii) 10 mM NaCl/9 mM KCl, (iv) 10 mM NaCl/90 mM, (v) 10 mM NaCl/450 mM KCl, (vi) 10 mM NaCl/900 mM KCl electrolyte. Inset showing the cell configuration. (B) Chronoamperometry data switching between +1 V and -1V. Inset showing the rectification ratio at +/-1 V. (C) and (D) As above, but with 100 mM $NaClO_4$ and (i) 30 mM NaCl/0.07 mM KCl, (ii) 30 mM NaCl/0.7 mM KCl, (iii) 30 mM NaCl/7 mM KCl, (iv) 30 mM NaCl/70 mM, (v) 30 mM NaCl/350 mM KCl, (vi) 30 mM NaCl/700 mM KCl electrolyte.

Chronoamperometry data and rectification plots (Figure 4B and 4D and insets) reveal effects from Na^+ in the KCl solution. The point at which inversion of the diode happens is shifted from ca. 9 mM KCl for 10 mM NaCl to about 70 mM KCl in the presence of 30 mM NaCl. A higher concentration of K^+ in the electrolyte is needed to reach the precipitaion point when Na^+ transport occurs in parallel. With increased Na^+ concentration, the currents in the positive (blocked) applied potential domain are still very low with only a stochastic spike noise indicating the presence of the $KClO_4$ blocking layer. Therefore, not only the K^+ ion flux is blocked but also the Na^+ flux across the heterojunction is blocked as one would expect for a physical barrier such as the $KClO_4$ precipitate.

As an analytical perspective, it is possible to consider the precipitation reaction in ionic diodes, for example for the detection or monitoring of K^+ concentration. Qualitatively, the presence of potassium is clearly revealed by the peak feature observed in the open state of the ionic diode. A change in K^+ concentration would be revealed by a shift in the peak. However, other cations such as Na^+ would affect the appearance of this peak and limit the amount of quantitative information that could be obtained. In order to extract more quantitative potassium concentration information (i) more selective ionomers need to be employed to only allow K^+ (as opposed to Na^+) transport, (ii) the time of dissolution of $KClO_4$ (e.g. monitored at zero current) could be employed assuming that the rate of $KClO_4$ dissolution should be external potassium concentration related, or (iii) a combination of two different microhole sizes (or two different ionic diode architectures with other materials) could be employed to give two subsequent blocking signals to analyse as independent signals. More exploratory work on similar devices and mechanisms but for other types of precipitation reactions will be required.

4. Conclusions

It has been shown that a PIM | Nafion-based interface in an ionic diode with “normal” cation flux characteristics can be blocked by precipitation to show “inverted” cation flux behavior. With K^+ accumulation in the presence of ClO_4^-, a near total ion flux blocking in the positive applied

potential domain occurs due to formation of a $KClO_4$ precipitate at the PIM-EA-TB | Nafion interface. This blocking effect is "physical" in the sense that transport of other cations such as Na^+ also gets blocked simultaneously.

In the future other precipitation mechanisms could be studied and the ionic diode device be made more selective to provide better sensitivity in electro-analytical detection applications. In a broader perspective, a wider range of "ionic diode mechanisms" could be studied and ionic diode architectures could be further developed to allow more functionality to evolve. Coupling of ion flow through the diode with chemical reactions would be desirable to mimic biological processes and to enable new energy conversion technologies.

Acknowledgements

B.R.P. thanks to Indonesian Endowment (LPDP RI) for a PhD scholarship. F.M and N.B.M. thanks the Leverhulme foundation for financial support (RPG-2014-308: "New Materials for Ionic Diodes and Ionic Photodiodes").

References

[1] Q.Y. Wang, B. Wu, C.X. Jiang, Y.M. Wang, T.W. Xu, Polymer interfaces Improving the water dissociation efficiency in a bipolar membrane with amino-functionalized MIL-101, J. Mem. Sci. 524 (2017) 370-376.

[2] C.H. Shen, R. Wycisk, P.N. Pintauro, High performance electrospun bipolar membrane with a 3D junction, Energ. Environm. Sci. 10 (2017) 1435-1442.

[3] A.Y. Mulkidjanian, K.S. Makarova, M.Y. Galperin, E.V. Koonin, Inventing the dynamo machine: The evolution of the F-type and V-type ATPases, Nature Rev. Microbiol. 5 (2007) 892-899.

[4] B. Riza Putra, B.D.B. Aaronson, E. Madrid, K. Mathwig, M. Carta, R. Malpass-Evans, N.B. McKeown, F. Marken, Ionic Diode Characteristics at a Polymer of Intrinsic Microporosity (PIM) | Nafion "Heterojunction" Deposit on a Microhole Poly(ethylene-terephthalate) Substrate, Electroanalysis (2017) DOI: 10.1002/elan.201700247.

[5] E. Madrid, P. Cottis, Y.Y. Rong, A.T. Rogers, J.M. Stone, R. Malpass-Evans, M. Carta, N.B. McKeown, F. Marken, Water desalination concept using an ionic rectifier based on a polymer of intrinsic microporosity (PIM), J. Mater. Chem. 3 (2015) 15849-15853.

[6] Y. Hou, Y. Zhou, L. Yang, Q. Li, Y. Zhang, L. Zhu, M.A. Hickner, Q.M. Zhang, Q. Wang, Flexible Ionic Diodes for Low-Frequency Mechanical Energy Harvesting, Adv. Energy Mater. 7 (2017) 1601983.

[7] W. Guo, Y. Tian, L. Jiang, Asymmetric Ion Transport through Ion-Channel-Mimetic Solid-State Nanopores, Acc. Chem. Res. 46 (2013) 2834-2846.

[8] H.G. Chun, T.D. Chung, Iontronics, Annual Review of Analytical Chemistry, R.G. Cooks, J.E. Pemberton, (Eds.), 8 (2015) 441-462.

[9] B. Lovrecek, A. Despic, J.O.M. Bockris, Electrolytic Junctions with Rectifying Properties, J. Phys. Chem. 63 (1059) 750-751.

[10] L. Hegedus, N. Kirschner, M. Wittmann, P. Simon, Z. Noszticzius, T. Amemiya, T. Ohmori, T. Yamaguchi, Nonlinear effects of electrolyte diodes and transistors in a polymer gel medium, Chaos, 9 (1999) 283-297.

[11] L. Hegedus, N. Kirschner, M. Wittmann, Z. Noszticzius, Electrolyte transistors: Ionic reaction-diffusion systems with amplifying properties, J. Phys. Chem. A 102 (1998) 6491-6497.

[12] W.H. Guan, S.X. Li, M.A. Reed, Voltage gated ion and molecule transport in engineered nanochannels: theory, fabrication and applications, Nanotechnol. 25 (2014) 122001.

[13] W.J. Lan, M.A. Edwards, L. Luo, R.T. Perera, X.J. Wu, C.R. Martin, H.S. White, Voltage-Rectified Current and Fluid Flow in Conical Nanopores, Acc. Chem. Res. 49 (2016) 2605-2613.

[14] T.S. Plett, W.J. Cai, M. Le Thai, I.V. Vlassiouk, R.M. Penner, Z.S. Siwy, Solid-State Ionic Diodes Demonstrated in Conical Nanopores, J. Phys. Chem. C 121 (2017) 6170-6176.

[15] H.J. Koo, O.D. Velev, Ionic current devices-Recent progress in the merging of electronic, microfluidic, and biomimetic structures, Biomicrofluidics 7 (2013) 031501.

[16] L.J. Cheng, L.J. Guo, Nanofluidic diodes, Chem. Soc. Rev. 39 (2010) 923-938.

[17] X. Hou, W. Guo, L. Jiang, Biomimetic smart nanopores and nanochannels, Chem. Soc. Rev. 40 (2011) 2385-2401.

[18] M. Ali, B. Yameen, J. Cervera, P. Ramirez, R. Neumann, W. Ensinger, W. Knoll, O. Azzaroni, Layer-by-Layer Assembly of Polyelectrolytes into Ionic Current Rectifying Solid-State Nanopores: Insights from Theory and Experiment, J. Amer. Chem. Soc. 132 (2010) 8338-8348.

[19] Y. Kong, X. Fan, M.H. Zhang, X. Hou, Z.Y. Liu, J. Zhai, L. Jiang, Nanofluidic Diode Based on Branched Alumina Nanochannels with Tunable Ionic Rectification, ACS Appl. Mater. Interfaces, 5 (2013) 7931-7936.

[20] K. Xiao, L. Chen, Z. Zhang, G.H. Xie, P. Li, X.Y. Kong, L.P. Wen, L. Jiang, A Tunable Ionic Diode Based on a Biomimetic Structure-Tailorable Nanochannel, Angew. Chem. Internat. Ed. 56 (2017) 8168-8172.

[21] G. Pérez-Mitta, A. Albesa, F.M. Gilles, M.E. Toimil-Molares, C. Trautmann, O. Azzaroni, Noncovalent Approach toward the Construction of Nanofluidic Diodes with pH-Reversible Rectifying Properties: Insights from Theory and Experiment, J. Phys. Chem. C, 121 (2017) 9070-9076.

[22] G. Pérez-Mitta, A.G. Albesa, C. Trautmann, M.E. Toimil-Molares, O. Azzaroni, Bioinspired Integrated Nanosystems based on Solid-state Nanopores: “Iontronic” Transduction of Biological, Chemical and Physical Stimuli, Chem. Sci., 8 (2017) 890-913.

[23] E. Madrid, Y.Y. Rong, M. Carta, N.B. McKeown, R. Malpass-Evans, G.A. Attard, T.J. Clarke, S.H. Taylor, Y.T. Long, F. Marken, Metastable Ionic Diodes Derived from an Amine-Based Polymer of Intrinsic Microporosity, Angew. Chem.-Internat. Ed. 53 (2014) 10751-10754.

[24] D.P. He, E. Madrid, B.D.B. Aaronson, L. Fan, J. Doughty, K. Mathwig, A.M. Bond, N.B. McKeown, F. Marken, A Cationic Diode Based on Asymmetric Nafion Film Deposits, ACS Appl. Mater. Interf. 9 (2017) 11272-11278.

[25] B.D.B. Aaronson, D.P. He, E. Madrid, M.A. Johns, J.L. Scott, L. Fan, J. Doughty, M.A.S. Kadowaki, I. Polikarpov, N.B. McKeown, F. Marken, Ionic Diodes Based on Regenerated alpha-Cellulose Films Deposited Asymmetrically onto a Microhole, ChemSelect 2 (2017) 871-875.

[26] B.D.B. Aaronson, D. Wigmore, M.A. Johns, J.L. Scott, I. Polikarpov, F. Marken, Cellulose Ionics: Switching Ionic Diode Responses by Surface Charge in Reconstituted Cellulose Films, Analyst (2017).

[27] Y.Y. Rong, Q.L. Song, K. Mathwig, E. Madrid, D.P. He, R.G. Niemann, P.J. Cameron, S.E.C. Dale, S. Bending, M. Carta, R. Malpass-Evans, N.B. McKeown, F. Marken, pH-induced reversal of ionic diode polarity in 300 nm thin membranes based on a polymer of intrinsic microporosity, Electrochem. Commun. 69 (2016) 41-45.

[28] N.B. McKeown, P.M. Budd, Exploitation of Intrinsic Microporosity in Polymer-Based Materials, Macromolecules 43 (2010) 5163-5176.

[29] N.B. McKeown, P.M. Budd, Polymers of intrinsic microporosity (PIMs): organic materials for membrane separations, heterogeneous catalysis and hydrogen storage, Chem. Soc. Rev. 35 (2006) 675-683.

[30] R.G.D. Taylor, C.G. Bezzu, M. Carta, K.J. Msayib, J. Walker, R. Short, B.M. Kariuki, N.B. McKeown, The Synthesis of Organic Molecules of Intrinsic Microporosity Designed to Frustrate Efficient Molecular Packing, Chem. Europ. J. 22 (2016) 2466-2472.

[31] C.Y. Li, A.L. Ward, S.E. Doris, T.A. Pascal, D. Prendergast, B.A. Helms, Polysulfide-Blocking Microporous Polymer Membrane Tailored for Hybrid Li-Sulfur Flow Batteries, Nano Lett. 15 (2015) 5724-5729.

[32] M. Carta, R. Malpass-Evans, M. Croad, Y. Rogan, M. Lee, I. Rose, N.B. McKeown, The synthesis of microporous polymers using Troger's base formation, Polymer Chem. 5 (2014) 5267-5272.

[33] M. Carta, R. Malpass-Evans, M. Croad, Y. Rogan, J.C. Jansen, P. Bernardo, F. Bazzarelli, N.B. McKeown, An Efficient Polymer Molecular Sieve for Membrane Gas Separations. Science 339 (2013) 303-307.

[34] M. Lee, C.G. Bezzu, M. Carta, P. Bernardo, G. Clarizia, J.C. Jansen, N.B. McKeown, Enhancing the Gas Permeability of Troger's Base Derived Polyimides of Intrinsic Microporosity, Macromolecules 49 (2016) 4147-4154.

[35] E. Tocci, L. De Lorenzo, P. Bernardo, G. Clarizia, F. Bazzarelli, N.B. Mckeown, M. Carta, R. Malpass-Evans, K. Friess, K. Pilnacek, M. Lanc, Y.P. Yampolskii, L. Strarannikova, V. Shantarovich, M. Mauri, J.C. Jansen, Molecular Modeling and Gas Permeation Properties of a Polymer of Intrinsic Microporosity Composed of Ethanoanthracene and Tröger's Base Units, Macromolecules 47 (2014) 7900-7916.

[36] gas storage.

[37] M. Carta, M. Croad, K. Bugler, K.J. Msayib, N.B. McKeown, Heterogeneous organocatalysts composed of microporous polymer networks assembled by Tröger's base formation, Polymer Chem. 5 (2014) 5262-5266.

[38] Y.Y. Rong, A. Kolodziej, E. Madrid, M. Carta, R. Malpass-Evans, N.B. McKeown, F. Marken, Polymers of intrinsic microporosity in electrochemistry: Anion uptake and transport effects in thin film electrodes and in free-standing ionic diode membranes, J. Electroanal. Chem. 779 (2016) 241-249.

[39] Y.Y. Rong, D.P. He, R. Malpass-Evans, M. Carta, N.B. McKeown, M.F. Gromboni, L.H. Mascaro, G.W. Nelson, J.S. Foord, P. Holdway, S.E.C. Dale, S. Bending, F. Marken, High-Utilisation Nanoplatinum Catalyst (Pt@cPIM) Obtained via Vacuum Carbonisation in a Molecularly Rigid Polymer of Intrinsic Microporosity, Electrocatalysis 8 (2017) 132-143.

[40] D.P. He, Y.Y. Rong, Z.K. Kou, S.C. Mu, T. Peng, R. Malpass-Evans, M. Carta, N.B. McKeown, F. Marken, Intrinsically microporous polymer slows down fuel cell catalyst corrosion, Electrochem. Commun. 59 (2015) 72-76.

[41] E. Madrid, D.P. He, J.L. Yang, C.F. Hogan, B. Stringer, K.J. Msayib, N.B. McKeown, P.R. Raithby, F. Marken, Reagentless Electrochemiluminescence from a Nanoparticulate Polymer of Intrinsic Microporosity (PIM-1) Immobilized onto Tin-Doped Indium Oxide, ChemElectroChem 3 (2016) 2160-2164.

[42] I. Chae, T. Luo, G.H. Moon, W. Ogieglo, Y.S. Kang, M. Wessling, Ultra-High Proton/Vanadium Selectivity for Hydrophobic Polymer Membranes with Intrinsic Nanopores for Redox Flow Battery, Adv. Energy Mater. 6 (2016) 1600517.

[43] K. Mathwig, B.D.B. Aaronson, F. Marken, Ionic Transport in Microhole Fluidic Diodes Based on Asymmetric Ionomer Film Deposits, CemElectroChem, (2017) DOI: 10.1002/celc.201700464.

[44] D.R. Lide (ed.), CRC Handbook of Chemistry and Physics, 74th edition, CRC Press, London, 1993-1994, p. 8-49.